East European Journal of Physics. 3. 131–145 (2025)
DOI: 10.26565/2312-4334-2025-3-12 ISSN 2312-4334

# HEAT AND MASS TRANSFER IN STRATIFIED MHD FLOW UNDER AN INCLINED MAGNETIC FIELD

**Mukul Medhi***, **Rudra Kanta Deka**
*Mathematics Department, Gauhati University, Guwahati-781014, Assam, India*
**Corresponding Author e-mail: mukulmedhi2@gmail.com*
Received May 6, 2025; revised June 6, 2025; accepted June 21, 2025

This study investigates how thermal and mass stratification influence unsteady magnetohydrodynamic fluid flow through a permeable medium over an inclined parabolic plate when a slanted magnetic field is present. Laplace transform method is used to find closed-form analytical benchmark solutions for flow governing equations. The study compares the results obtained from thermal and mass stratification with scenarios where both forms of stratification are not present. Non-stratified cases demonstrate elevated velocities in comparison. Also the presence of both stratifications increases skin friction by 33.42%, the heat transfer rate by 97.54%, and the mass transfer rate by 36.91%. The biggest influence on fluid flow arises when the magnetic field is orthogonal to the flow direction. This study's conclusions are pertinent for optimising fluid dynamics in engineering and environmental applications.

**Keywords:** *MHD; Porous medium; Parabolic inclined plate; Thermal Stratification; Mass Stratification; Inclined magnetic field*

**PACS:** 44.05.+e, 47.11.-j, 47.65.-d, 47.56.+r

## Nomenclature

| | |
|---|---|
| $\alpha$ | Thermal diffusivity ($m^2/s$) |
| $\beta$ | Volumetric coefficient of thermal expansion ($1/K$) |
| $\gamma'$ | Thermal stratification parameter |
| $\gamma$ | Dimensionless thermal stratification parameter |
| $\lambda$ | Inclination angle of the plate |
| $\phi$ | Angle of inclination of magnetic field |
| $\nu$ | Kinematic viscosity ($m^2/s$) |
| $\sigma$ | Electrical conductivity. ($1/ohm.m$) |
| $\tau$ | Non-dimensional skin friction |
| $\xi'$ | Mass stratification parameter |
| $\xi'$ | Dimensionless mass stratification parameter |
| $C$ | Non-dimensional concentration |
| $C'$ | Species concentration in the fluid ($mol/m^3$) |
| $C'_\infty$ | Concentration far from the plate ($mol/m^3$) |
| $C'_w$ | Concentration at the plate ($mol/m^3$) |
| $D$ | Mass diffusion coefficient ($m^2/s$) |
| $g$ | Gravitational acceleration ($m/s^2$) |
| $Gc$ | Mass Grashof number |
| $\beta^*$ | Expansion coefficient with concentration ($m^2/h$) |
| $Gr$ | Thermal Grashof number |
| $Nu$ | Nusselt number |
| $Pr$ | Prandtl number |
| $t$ | Non-dimensional time |
| $T'$ | Temperature of the fluid (K) |
| $t'$ | Time (s) |
| $T'_\infty$ | Temperature far from the plate (K) |
| $T'_w$ | Temperature at the plate (K) |
| $T$ | Non-dimensional temperature |
| $k'_p$ | Dimensional permeability |
| $k_p$ | Permeability |
| $u$ | Non-dimensional velocity |
| $u'$ | Velocity in $x$ direction ($m/s$) |
| $u_0$ | Reference velocity |
| $b'$ | Dimensional acceleration parameter |

***Cite as:*** M. Medhi, R.K. Deka, East Eur. J. Phys. 3, 131 (2025), https://doi.org/10.26565/2312-4334-2025-3-12

| | |
|---|---|
| $b$ | Accelerating parameter |
| $y'$ | Non-dimensional coordinate normal to the plate |
| $y$ | Dimensional coordinate normal to the plate (m) |
| $B_0$ | Magnetic field strength |
| $M$ | Magnetic parameter |

## 1. INTRODUCTION

MHD focusses on the interaction of magnetic fields with electrically conducting fluids in motion. MHD exhibits application across a range of disciplines, encompassing plasma physics, astrophysics, and the design of MHD generators and pumps. Beyond the areas already mentioned, it holds immense potential across a broad spectrum of disciplines, including aeronautics, chemical engineering, electrical engineering, medicine, and the biological sciences. The field of magnetohydrodynamics was pioneered by the prominent Swiss physicist Hannes Alfvén [1]. Significant contributions from scholars such as [2], [3], [4], and [5] have shaped the current state of MHD. [6] investigated how MHDs are used practically in biological systems. According to [7], one of the most vital uses of MHD is the pumping of materials that are challenging to pump using ordinary pumps. [8] conducted a numerical investigation of the electroosmotic-driven transport of MHD Casson fluid via an exponential stretching sheet. Recent academic investigations by scholars including [9], [10], [11], [12], [13], [14], [15], [16], [17] and [18] have explored magnetohydrodynamic flows across a range of geometric contexts.

A material characterised by voids or pore spaces, devoid of solid, contained inside a solid or semisolid matrix is referred to as porous material. The permeability of porous materials is a defining characteristic, enabling the passage of various fluids from one side to the other. As a result, these materials are prevalent in both natural and technological contexts. Numerous fields, including hydrology and petroleum engineering, rely extensively on porous media. Consequently, the study of fluid dynamics within porous environments has garnered significant scholarly attention. A model addressing the boundary conditions of a porous material in relation to viscous fluid flow around a porous solid has been examined by [19] and [20]. [21] examined the heat generation and chemical reaction impact on MHD flow of Jeffrey nanofluid through a porous medium. It was examined by [22] how thermal radiation and chemical reactions affected Williamson MHD fluid flow embedded in porous environment. [23] conducted an analytical examination of the impacts of Soret effect and thermal generation on the unsteady magnetohydrodynamic flow of radiating and electrically conducting nanofluid across an oscillating vertical plate within a porous media. Furthermore, the subsequent researchers, [24], [25], [26], [27] and [28] are extensively engaged in the investigation of porous medium transport phenomena.

An inclined magnetic field serves as an important factor, especially in industrial applications and biological studies.Between 0 and 90 degrees is the range of this magnetic field's inclination angle. The impact of a tilted magnetic field on hydromagnetic flow across an oblique oscillating plate and a linearly accelerating plate was examined by [29] and [30]. [31] examined the influence of an angled magnetic field on the time-dependent squeezing flow between parallel plates with suction and injection. [32] investigated the flow and temperature distribution of MHD Casson fluid via a permeable extended surface within laminar flow regime. The unsteady hydro magnetic couette flow in the presence of a variable inclined magnetic field was analysed by [33]. The study of heat and mass transfer in unstable magnetohydrodynamic flow in two non-conducting infinite vertical plates with an slanted magnetic field is studied by [34]. In a perforated medium with a changing temperature, an angled magnetic field, and stable mass diffusion, [35] examined unsteady free-convection MHD fluid flow in conjunction with an exponentially accelerating plate. [36] investigated time variation measurements by the influence of Dufour, Hall, and ion-slip currents in unsteady magneto-hydrodynamic fluid flow across an inclined plate with an inclined generated magnetic field.

Research on MHD flow problems related to the motion induced by the sudden initiation of endless vertical plates exhibiting parabolic velocity has been extensively conducted, owing to their prospective uses in domains like astrophysics, geophysics, and missile technology. [37], [38], [39], and [40] are among them. [41] started their research by examining parabolic flow over an upright plate with uniform heat flux and variable mass diffusion, establishing a foundation for comprehending such intricate fluid dynamics. [42] recently conducted a numerical study on the MHD fluid's parabolic flow via an upright plate in a porous medium. [43] has examined the issue of the effects of a angled magnetic field on a transit radiative hydromagnetic flow across an oblique parabolic accelerating plate inside a porous medium, including chemical reactions and heat-generating parameters. Further [44] extended this by considering thermal diffusion effect. [45] examined how radiation and Hall current, in addition to a changing temperature, affected MHD flow over an inclined parabolic accelerating plate through a porous media. When rotation and the first chemical substance reaction were present, [46] examined parabolic flow via an isothermal perpendicular plate with heat and mass scattering.

None of the studies mentioned previously included thermal and mass stratification, which is crucial for weather and climatic prediction, comprehension of natural systems, engineering applications, and environmental and safety aspects. In the complex realm of fluid dynamics, thermal stratification and mass stratification are crucial factors. Thermal Stratification arises from resistance to heat transport, resulting in discrete layers within a fluid, whereas Mass Stratification occurs owing to density variations caused by differing solute concentrations. [47] and [48] developed analytical solutions for unsteady flow across an endless upright plate under various surface conditions. [49] and [50] investigated the impacts of mass and

thermal stratification on a upright wavy truncated cone and a wavy vertical surface within saturated porous media of a non-Newtonian fluid. [51] established the analytical solution for the simultaneous influences of mass and thermal stratification on unsteady flow via exponential mass diffusion and an accelerating plate inside a porous medium exhibiting variable temperatures. [52] examined the unsteady parabolic flow in a porous media over an endless upright plate, characterized by exponential temperature decay and variable mass diffusion, considering the effects of thermal and mass stratification. [53] and [54] developed solutions addressing the impacts of mass and thermal stratification on unsteady magnetohydrodynamic flow under various surface conditions.

Inspired by the aforementioned literary works, we endeavoured to conduct a precise examination of the matter concerning the effects of a slanted magnetic field, as well as thermal and mass stratification, on a transit hydromagnetic flow over a tilted parabolic accelerated plate within a porous medium. Based on the authors' knowledge, no studies have been conducted on the impact of inclined magnetic field, thermal and mass stratification on hydromagnetic flow past a parabolic accelerating inclined plate through a porous media. So, the novelty of concepts and physical facts presented in this study is anticipated to significantly influence and facilitate interactions across many domains. This problem is resolved in a closed form with a potent method, namely the Laplace transform approach. Subsequently, the results for the fluid with two stratifications are contrasted with those for the specific scenario devoid of stratification. The effects of various physical entities on the non-dimensional velocity of fluid, temperature distribution, fluid concentration, shear stress, and rates of heat and mass transfer are illustrated graphically and through tabulated data. The practical relevance of this study's conclusions pertains to the optimization of fluid dynamics in engineering and environmental applications. Both stratification's effects on magnetohydrodynamic flow in porous media may increase the effectiveness of mass transfer and heat transfer systems, which can be used in energy system design, industrial cooling, and pollution control.

## 2. MATHEMATICAL FORMULATION

Consider the unsteady MHD flow of a viscous, incompressible, stratified fluid past an inclined parabolic accelerated plate within the porous medium. We employ a rectangular Cartesian coordinate system in which the $y$ -axis is orthogonal to the plate and the $x$ -axis extends uprightly along the plate. The magnetic field vector affecting the flow is given by $B = (B_0 \cos\phi, B_0 \sin\phi, 0$ when a constant magnetic field $B_0$ is applied at an arbitrary angle $\phi$ with the axis $x$. Furthermore, the plate is intended to be inclined at an arbitrary angle $\lambda$. Both inclinations are expected to be oriented vertically. At the initial time ($t' = 0$), the plate is stationary. However, the plate begins to move parabolically with velocity $u' = u_0(b't'^2)$ in its own plane at $t' > 0$. Due to the infinite length of the plate, all flow variables are independent of $x$ and depend solely on $y$ and $t'$. The induced magnetic field is to be disregarded due to the consideration of a very small magnetic Reynolds number. Furthermore, it is considered that the viscous dissipation of energy is negligible. Figure 1 clearly illustrates the geometry of the problem.

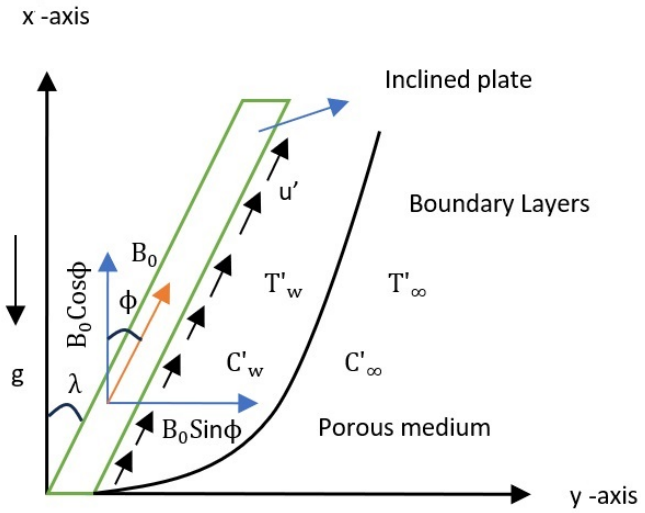


**Figure 1.** Flow geometry .

Consequently, according to Boussinesq's approximation, the equations delineated in refs [43], [44] and [52] are employed to characterise the unsteady flow.

$$\frac{\partial u'}{\partial t'} = g\beta(T' - T'_\infty)\cos\lambda + g\beta^*(C' - C'_\infty)\cos\lambda + \nu\frac{\partial^2 u'}{\partial y^2} - \left(\frac{\sigma\beta_0^2\sin^2\phi}{\rho} + \frac{\nu}{k'_p}\right)u' \tag{1}$$

$$\frac{\partial T^{'}}{\partial t^{'}} = \alpha \frac{\partial^2 T^{'}}{\partial y^2} - \gamma^{'} u^{'} \tag{2}$$

$$\frac{\partial C^{'}}{\partial t^{'}} = D \frac{\partial^2 C^{'}}{\partial y^2} - \xi^{'} u^{'} \tag{3}$$

with following initial and boundary condition [44] and [55]:

$$\begin{gathered} t^{'} \leq 0: \quad u^{'} = 0, \quad T^{'} = T_{\infty}^{'}, \quad C^{'} = C_{\infty}^{'}, \quad \forall \quad y \\ t^{'} > 0: \quad u^{'} = u_0(b^{\prime} t^{\prime 2}), \quad T^{'} = T_{w}^{'}, \quad C^{'} = C_{w}^{'} \quad at \quad y = 0 \\ u^{'} \to 0, \quad T^{'} \to T_{\infty}^{'}, \quad C^{'} \to C_{\infty}^{'} \quad as \quad y \to \infty \end{gathered} \tag{4}$$

where "thermal stratification parameter" and "mass stratification paramter are termed as $\gamma^{\prime} = \frac{dT_{\infty}^{'}}{dx} + \frac{g}{C_p}$ and $\xi^{'} = \frac{dC_{\infty}^{'}}{dx}$. The phrase "thermal stratification" denotes the interplay of vertical temperature advection $\left(\frac{dT_{\infty}^{'}}{dx}\right)$, wherein the temperature of the surrounding fluid is height-dependent, and the work of compression $\left(\frac{g}{C_p}\right)$ represents the rate at which particles in a fluid perform reversible work as a result of compression.

Introducing dimensionless variables:

$$\begin{gathered} u = \frac{u^{\prime}}{u_0}, \quad t = \frac{t^{\prime} u_0^2}{\nu}, \quad y^{'} = \frac{u_0 y}{\nu}, \quad C = \frac{C^{'} - C_{\infty}^{'}}{C_{w}^{'} - C_{\infty}^{'}}, \quad \theta = \frac{T^{'} - T_{\infty}^{'}}{T_{w}^{'} - T_{\infty}^{'}}, \\ Gr = \frac{g\beta\nu(T_{w}^{\prime} - T_{\infty}^{\prime})}{u_0^3}, \quad M = \frac{\sigma\beta_0^2\nu}{\rho u_0^2}, \quad Gc = \frac{g\beta^{*}\nu(C_{w}^{\prime} - C_{\infty}^{\prime})}{u_0^3}, \quad Sc = \frac{\nu}{D} \\ k_p = \frac{k_p^{\prime} u_0^2}{\nu^2}, \quad \gamma = \frac{\gamma^{\prime}\nu}{u_0(T_{w}^{'} - T_{\infty}^{'})}, \quad \xi = \frac{\xi^{\prime}\nu}{u_0(C_{w}^{'} - C_{\infty}^{'})}, \quad Pr = \frac{\nu}{\alpha}, \quad b = \frac{b^{\prime}\nu^2}{u_0^4} \end{gathered} \tag{5}$$

The transformed governing equation in dimensionless form are:

$$\frac{\partial u}{\partial t} = \frac{\partial^2 u}{\partial y^{\prime 2}} + Gr\, T \cos\lambda + Gc\, C \cos\lambda - \left(M\, \sin^2\phi + \frac{1}{k_p}\right) u \tag{6}$$

$$\frac{\partial \theta}{\partial t} = \frac{1}{Pr} \frac{\partial^2 \theta}{\partial y^{\prime 2}} - \gamma\, u \tag{7}$$

$$\frac{\partial C}{\partial t} = \frac{1}{Sc} \frac{\partial^2 C}{\partial y^{\prime 2}} - \xi\, u \tag{8}$$

and the dimensionless initial and boundary constraints are:

$$\begin{gathered} t \leq 0: \quad u = 0, \quad \theta = 0, \quad C = 0 \quad \forall \quad y^{'} \\ t > 0: \quad u = b\, t^2, \quad \theta = 1, \quad C = 1 \quad at \quad y^{'} = 0 \\ u \to 0, \quad \theta \to 0, \quad C \to 0 \quad as \quad y^{'} \to \infty \end{gathered} \tag{9}$$

## 3. METHOD OF SOLUTION

The use of the Laplace transform method yields an equation of non-tractable form for any given Prandtl or Schmidt number. The non-dimensional governing equations from (6) to (8) , along with the boundary conditions (9), are solvable when the conditions are reduced to $Pr = 1$, $Sc = 1$. Consequently, we get

$$\frac{d^2\overline{u}}{dy^{\prime 2}} - \left(s + h_1\right)\overline{u} + Gr\, \overline{T}\, \cos\lambda + Gc\, \overline{C}\, \cos\lambda = 0 \tag{10}$$

$$\frac{d^2\overline{T}}{dy^{\prime 2}} - s\, \overline{T} - \gamma\, \overline{u} = 0 \tag{11}$$

$$\frac{d^2\overline{C}}{dy^{\prime 2}} - s\, \overline{C} - \xi\, \overline{u} = 0 \tag{12}$$

where $h_1 = M\, \sin^2\phi + \frac{1}{k_p}$ and $s$ denotes the Laplace transform parameter.

This set of ordinary differential equations is solved alongside the initial boundary conditions, employing the inverse Laplace transform technique as facilitated by [56] and [57] . Consequently, we derive the subsequent profiles of velocity, temperature, and concentration:

$$u = \frac{2\,b}{h_3}\left(h_4\,L_2(h_4) - h_5\,L_2(h_5)\right) + \frac{h_6}{h_3}\left(L_1(h_5) - L_1(h_4)\right) \tag{13}$$

$$\theta = \frac{(\xi-\gamma)\,Gc\,\cos\phi}{h_5 h_4} erfc\left(\frac{y^{'}}{2\sqrt{t}}\right) + \frac{2\,\gamma\,b}{h_3}\left(L_2(h_4) - L_2(h_5)\right) + \frac{\gamma\,h_6}{h_3}\left(\frac{L_1(h_5)}{h_5} - \frac{L_1(h_4)}{h_4}\right) \tag{14}$$

$$C = \frac{(\gamma-\xi)\,Gr\,\cos\phi}{h_5 h_4} erfc\left(\frac{y^{'}}{2\sqrt{t}}\right) + \frac{2\,\xi\,b}{h_3}\left(L_2(h_4) - L_2(h_5)\right) + \frac{\xi\,h_6}{h_3}\left(\frac{L_1(h_5)}{h_5} - \frac{L_1(h_4)}{h_4}\right) \tag{15}$$

where

$$h_2 = Gr\,\gamma\,\cos\phi + Gc\,\xi\,\cos\phi, \quad h_3 = \sqrt{h_1^2 - 4h_2}, \quad h_4 = \frac{h_1+h_3}{2}, \quad h_5 = \frac{h_1-h_3}{2}$$
$$h_6 = Gr\,\cos\phi + Gc\,\cos\phi$$

$L_i^{'}s$ indicate inverse Laplace's transforms as stated below

$$L_1(p) = L^{-1}\left\{\frac{e^{-y^{'}\sqrt{s+p}}}{s}\right\}, \quad L_2(p) = L^{-1}\left\{\frac{e^{-y^{'}\sqrt{s+p}}}{s^3}\right\},$$

## 4. CLASSICAL CASE ($\gamma = 0$, $\xi = 0$)

Solutions have been derived for the unique scenario in which stratification is absent. We aim to compare the outcomes of the fluid exhibiting thermal and mass stratification with the scenario devoid of stratification. Therefore, the solutions for the classical scenario with boundary conditions (9) via the Laplace transformation are as follows:

$$\theta_c = erfc\left(\frac{y^{'}}{2\sqrt{t}}\right) \tag{16}$$

$$C_c = erfc\left(\frac{y^{'}}{2\sqrt{t}}\right) \tag{17}$$

$$u_c = 2\,b\,L_2(h_1) - \frac{h_6}{h_1}L_1(h_1) + \frac{h_6}{h_1}\,erfc\left(\frac{y^{'}}{2\sqrt{t}}\right) \tag{18}$$

### Skin Friction

We obtained the non-dimensional skin-friction from the velocity field, which represents the shear stress at the surface, as follows:

$$\tau = -\left.\frac{\partial u}{\partial y^{'}}\right|_{y^{'}=0}$$

$$= \frac{2\,b}{h_3}\left(h_4\,g_2(h_4) - h_5\,g_2(h_5)\right) + \frac{h_6}{h_3}\left(g_1(h_5) - g_1(h_4)\right) \tag{19}$$

Skin Friction for special case:

$$\tau_c = -\left.\frac{\partial u_c}{\partial y^{'}}\right|_{y^{'}=0}$$

$$= 2\,b\,g_2(h_1) - \frac{h_6}{h_1}g_1(h_1) + \frac{h_6}{h_1}\left(\frac{1}{\sqrt{\pi}\,\sqrt{t}}\right) \tag{20}$$

**Nussely Number**

We obtained the non-dimensional Nusselt number from the temperature field, which represents the rate of heat transfer, as follows:

$$Nu = -\frac{\partial \theta}{\partial y'}\bigg|_{y'=0}$$

$$= \frac{(\xi - \gamma)\, Gc\, \cos\phi}{h_5 h_4}\left(\frac{1}{\sqrt{\pi}\,\sqrt{t}}\right) + \frac{2\,\gamma\, b}{h_3}\Big(g_2(h_4) - g_2(h_5)\Big) + \frac{\gamma\, h_6}{h_3}\left(\frac{g_1(h_5)}{h_5} - \frac{g_1(h_4)}{h_4}\right) \tag{21}$$

Nusselt number for special case:

$$Nu_c = -\frac{\partial \theta_c}{\partial y'}\bigg|_{y'=0}$$

$$= \frac{1}{\sqrt{\pi}\,\sqrt{t}} \tag{22}$$

**Sherwood Number**

We obtained the non-dimensional Sherwood number from the concentration field, which represents the rate of mass transfer, as follows:

$$Sh = -\frac{\partial C}{\partial y'}\bigg|_{y'=0}$$

$$= \frac{(\gamma - \xi)\, Gr\, \cos\phi}{h_5 h_4}\left(\frac{1}{\sqrt{\pi}\,\sqrt{t}}\right) + \frac{2\,\xi\, b}{h_3}\Big(g_2(h_4) - g_2(h_5)\Big) + \frac{\xi\, h_6}{h_3}\left(\frac{g_1(h_5)}{h_5} - \frac{g_1(h_4)}{h_4}\right) \tag{23}$$

Sherwood number for special case:

$$Sh_c = -\frac{\partial C_c}{\partial y'}\bigg|_{y'=0}$$

$$= \frac{1}{\sqrt{\pi}\,\sqrt{t}} \tag{24}$$

where,

$$g_1(x) = \frac{e^{-x\,t}}{\sqrt{\pi\, t}} + \sqrt{x}\, erf(\sqrt{x\, t})$$

$$g_2(x) = \frac{(4tx(tx+1) - 1)\, erf\left(\sqrt{tx}\right)}{8x^{3/2}} + \frac{\sqrt{t}e^{-tx}(2tx+1)}{4\sqrt{\pi}x}$$

## 5. RESULTS AND DISCUSSION

Utilising the solutions established in earlier sections, we computed numerical values for a range of physical parameters, including concentration, skin friction, velocity, temperature, and Nusselt and Sherwood number. This study enabled us to explore the physical dimensions of the problem more thoroughly. Additionally, we used MATHEMATICA to generate plots shown in Figures 2-26. This research considers the following parameters: $M = 1$, $k_p = 0.5$, $Gr = 5$, $Gc = 5$, $t = 2$, $b = 0.2$, $y' = 1.5$, $\gamma = 0.5$, $\xi = 0.3$, $\phi = \frac{\pi}{3}$, $\theta = \frac{\pi}{3}$. Parameters ranges are: $0 \le \gamma \le 1$, $0 \le \xi \le 1$, $2 \le Gr \le 10$, $2 \le Gc \le 10$, $0.5 \le k_p \le 2.3$, $0.5 \le M \le 5$, $\frac{\pi}{9} \le \phi \le \frac{\pi}{2}$, $\frac{\pi}{9} \le \lambda \le \frac{\pi}{3}$, $0.1 \le b \le 0.4$. To validate the accuracy of the the approach, the temperature profile produced by [55] is juxtaposed with the temperature profile derived from the scenario of no thermal stratification, as seen in Figure 2. The findings are in strong agreement.

Graphs showing the impacts of $\gamma$ and $\xi$ on the velocity, temperature, and concentration profile are shown in Figures 3, 10, and 17. Thermal and mass stratification lowers the flow velocity, as seen in Figure 3. As the stratification parameters ($\gamma$, &, $\xi$) rise, the convective interaction between the ambient fluid and the hot plate falls. Because of this reduction in buoyancy force, the flow velocity therefore decreases. Figure 10 illustrates that the classical scenario has a greater temperature compared to the nonclassical circumstance. It illustrates that temperature increases owing to mass stratification, but decreases due to thermal stratification. The temperature difference between the vertical plate and the surrounding fluid diminishes in the presence of thermal stratification. This results in an increase in the thickness of the heat boundary layer, hence reducing the temperature. Figure 17 demonstrates that fluid concentration increases with a higher thermal stratification parameter, while it decreases with an increasing mass stratification parameter.

Graphs showing the influences of $Gr$ and $Gc$ on the velocity, temperature, and concentration profile are shown in Figures 4, 11, and 18. Figure 4 shows that when both Grashof numbers increase, the velocity profiles also increase,

which is because the buoyancy force is directly proportional to the Grashof numbers. Figure 11 shows that temperature decreases as $Gr$ and $Gc$ increase, suggesting that heat dissipation away from the heated surface is increased by improved buoyancy-driven fluid flow. The impacts of $Gr$ and $Gc$ on concentration have been shown to be identical to those seen for Figure 18's temperature profiles.

Graphs showing the effect of $k_p$ on the velocity, temperature, and concentration profile are shown in Figures 5, 12, and 19. Permeability, determined by the geometry of the medium rather than the characteristics of the fluid. It quantifies formation's ability to transmit fluids, directly relating to the interconnectedness of pores, which influences fluid movement within the medium. The larger the interconnectedness of void spaces, the more easily fluid can traverse the medium. Hence, the increase in medium permeability results in enhanced fluid flow. Consequently, the velocity field increases with larger pore sizes in the medium, as illustrated in the provided Figure 5. Figures 12 and 19 indicate that temperature and concentration diminish as the permeability parameter elevates. This occurs as the pore sizes in the medium increases, allowing for greater mobility of the fluid's particles.

Graphs showing the influence of $M$ on the velocity, temperature, and concentration profile are shown in Figures 6, 13, 20. In the study of magnetohydrodynamic (MHD) flow, the Lorentz force has a prominent influence on the motion of particles of an electrically conducting fluid, naturally tending to diminish fluid velocity. The Lorentz force is exactly proportional to the magnetic field. Consequently, when the magnetic field intensifies, the resistance to fluid motion inside the flow domain escalates. Hence, velocity profiles decrease as $M$ increases, as seen in Figure 6. Furthermore, as M is increased, the temperature rises as shown in Figure 13. Because of improved confinement, resistive heating, suppression of cooling systems, and higher energy absorption from the field, an increase in $M$ usually causes a rise in temperature. Figure 20 illustrates how $M$ affects the concentration profile. The figure shows that the concentration of shear layers is improved by elevating $M$. This is caused by the Lorentz force, which opposes the direction of flow as the intensity of the magnetic field rises.

Graphs showing the effect of $\phi$ on the velocity, temperature, and concentration profile are shown in Figures 7, 14, and 21. Figure 7 illustrates the impact of an arbitrary magnetic field inclination angle on nondimensional velocity. It is evident that a rise in the tilt of the magnetic field results in a drop in fluid velocity. This occurs because the resistive force, known as the Lorentz force, intensifies with an elevated in the inclination angle. When the direction of the magnetic field is orthogonal to the flow of the fluid, it has the greatest impact on the flow. However, increase in $\phi$ escalates temperature and concentration profile of the fluid as seen in Figures 14, and 21.

Graphs showing the impact of $\lambda$ on the velocity, temperature, and concentration profile are shown in Figures 8, 15, and 22. As the plate's inclination angle rises, we can see that the fluid flow decreases. It is well known that the frictional force acting on the fluid dramatically rises across the flow domain when the plate is angled with respect to the flow direction. The provided Figure 8 illustrates how this physical fact results in a drop in fluid velocity. However, rise in $\lambda$ escalates temperature and concentration profile of the fluid as seen in Figures 15, and 22.

Graphs showing the effect of $b$ on the velocity, temperature, and concentration profile are shown in Figures 9, 16, and 23. Figure 9 shows that velocity increases as b increases. This is due to the fact that a stronger propulsive force applied on the fluid is implied by an increase in acceleration. Figure 16 illustrates how temperature drops as $b$ increases. The way that acceleration affects the fluid's energy distribution helps to understand this tendency. Increased acceleration imparts additional kinetic energy to the fluid, especially in the vicinity of the surface, which is converted to thermal energy via fluid friction and viscous dissipation. By increasing the base temperature throughout the fluid, this improved energy conversion raises the system's minimum temperature. Also concentration profile decreases as rise in $b$ as seen in Figure 23.

Graphs showing the effect of $\gamma$ and $\xi$ on the Skin Friction, Nusselt Number and Sherwood Number are shown in Figures 24, 25, and 26. In Figure 24, the skin friction curve shows a noticeable increase over time, especially in cases where both thermal ($\gamma$) and mass ($\xi$) stratification are present. In contrast to the scenario devoid of stratification, the upward trend signifies that the combined effect of temperature and mass stratification amplifies the fluid's resistance over the surface, resulting in elevated skin friction. Figures 25 and 26 illustrate an upward trend in the Nusselt and Sherwood values over time, suggesting enhanced mass and heat transmission. The increase is more significant with higher values of thermal stratification ($\gamma$) and mass stratification ($\xi$), as seen by the steeper curves. This behaviour indicates that enhanced stratification significantly improves the efficiency of heat and mass transfer in the fluid.

Table 1 shows how different parameters affect Skin friction ($\tau$), Nusselt number ($Nu$), and Sherwood number ($Sh$). When the magnetic parameter ($M$) increases, the skin friction also increases because the magnetic force resists the fluid flow by inducing the Lorentz force, this also reduces heat and mass transfer, lowering $Nu$ and $Sh$. On the other hand, increasing the permeability of the medium ($k_p$) allows the fluid to pass through more easily, which reduces skin friction but improves heat and mass transfer. Higher values of the thermal and mass Grashof numbers ($Gr$ and $Gc$) increase $Nu$ and $Sh$, showing stronger buoyancy-driven flow. But very high values can cause flow reversal near the plate, which lowers skin friction. Changing the angles of the magnetic field ($\phi$) and the plate ($\lambda$) slightly reduces skin friction while helping heat and mass transfer. Finally, increasing the acceleration parameter ($b$) increases all three values, showing that unsteady motion boosts shear stress and improves both heat and mass transfer. Table 2 indicates that the presence of both stratifications increases skin friction by 33.42%, the heat transfer rate by 97.54%, and the mass transfer rate by 36.91%.

The Nusselt number ($Nu$) represents the ratio of convective to conductive heat transfer across a fluid boundary and is a fundamental parameter in the analysis of thermal transport phenomena. Similarly, the Sherwood number ($Sh$) quantifies the ratio of convective to diffusive mass transfer, serving as its mass transfer analogue. These dimensionless numbers

are critical in characterizing transport processes and evaluating the influence of various physical effects, such as thermal and solutal stratification or magnetohydrodynamic (MHD) forces. A detailed analysis of Nu and Sh provides insights into the enhancement or suppression of energy and mass transport under complex flow conditions. In practical systems, such understanding supports the optimization of engineering applications including heat exchangers, chemical processing units, and environmental control systems. Therefore, exploring the interplay between convective transport mechanisms and external effects is essential for the development of more efficient and purpose-specific thermal and mass transfer systems.

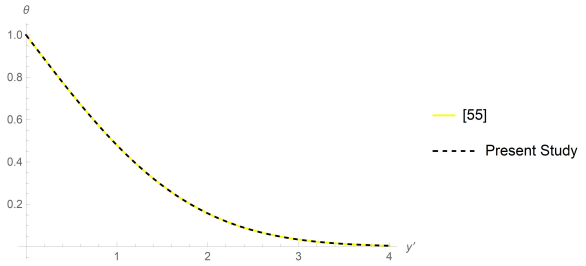


**Figure 2.** Comparison of temperature profile in the absence of $\gamma$

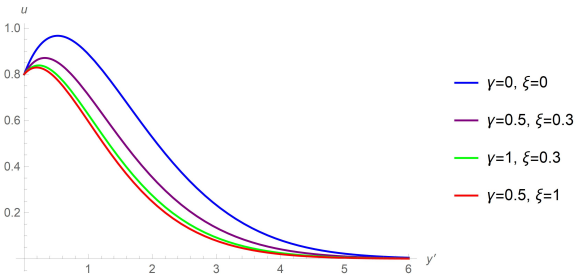


**Figure 3.** Effects of $\gamma$ & $\xi$ on velocity profile

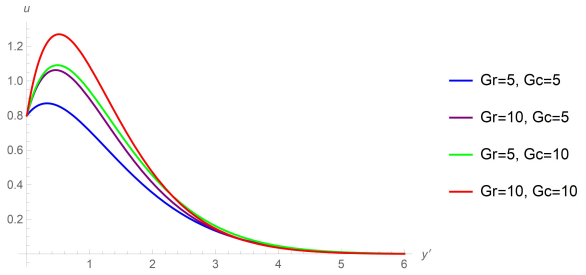


**Figure 4.** Effects of $Gr$ & $Gc$ on velocity profile

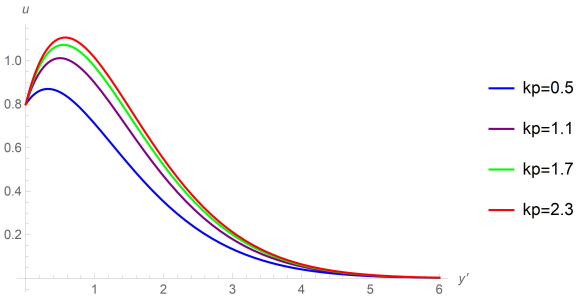


**Figure 5.** Effect of $k_p$ on velocity profile

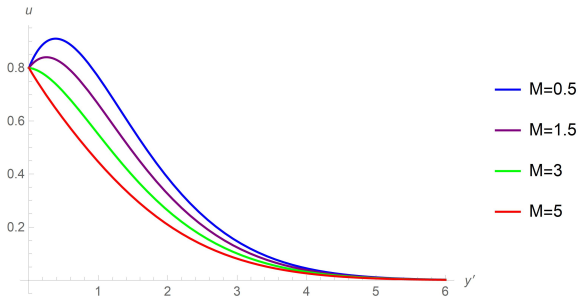


**Figure 6.** Effect of $M$ on velocity profile

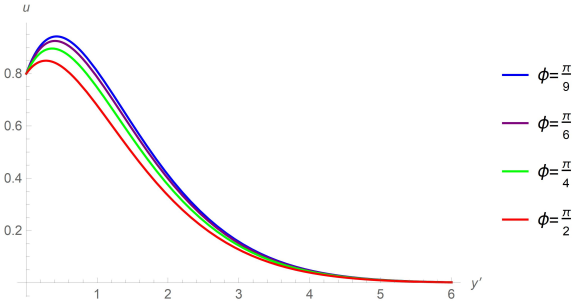


**Figure 7.** Effect of $\phi$ on velocity profile

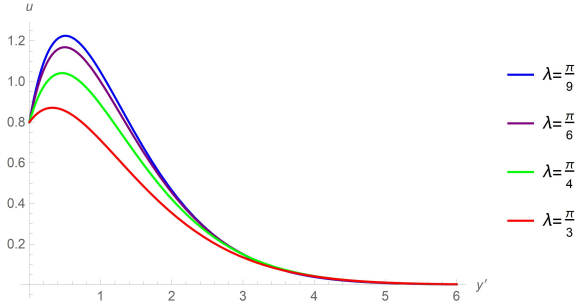


**Figure 8.** Effect of $\lambda$ on velocity profile

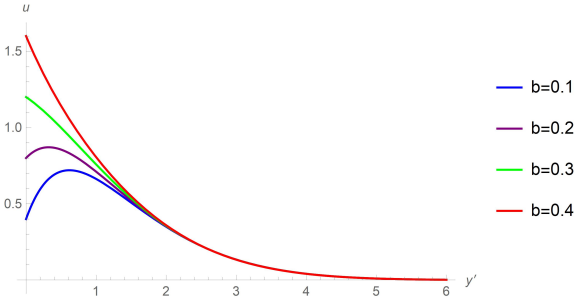


**Figure 9.** Effect of $b$ on velocity profile

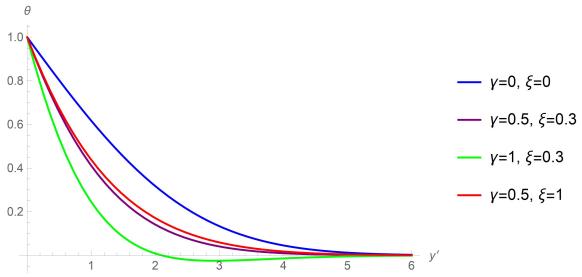


**Figure 10.** Effects of $\gamma$ & $\xi$ on temperature profile

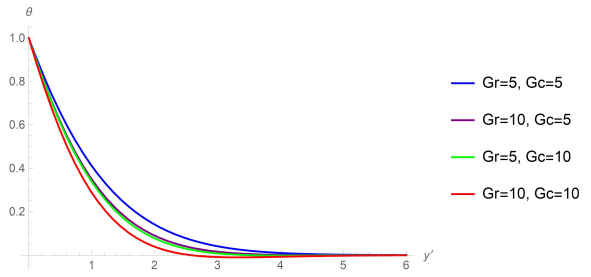


**Figure 11.** Effects of $Gr$ & $Gc$ on temperature profile

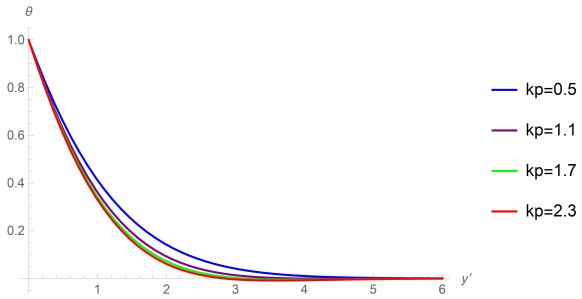


**Figure 12.** Effect of $k_p$ on temperature profile

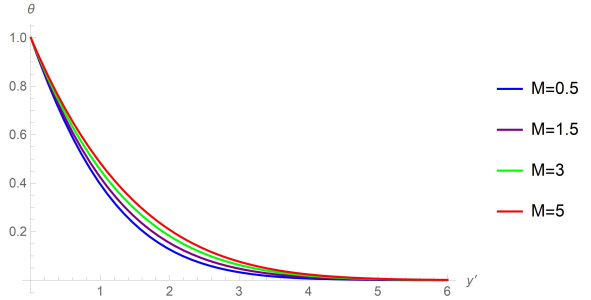


**Figure 13.** Effect of $M$ on temperature profile

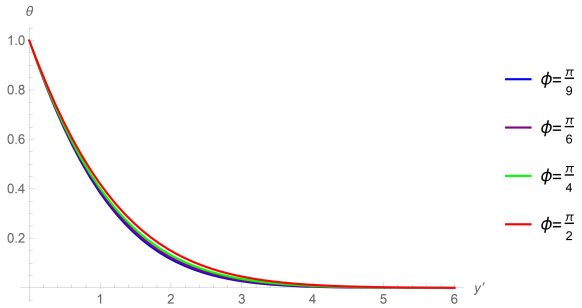


**Figure 14.** Effect of $\phi$ on temperature profile

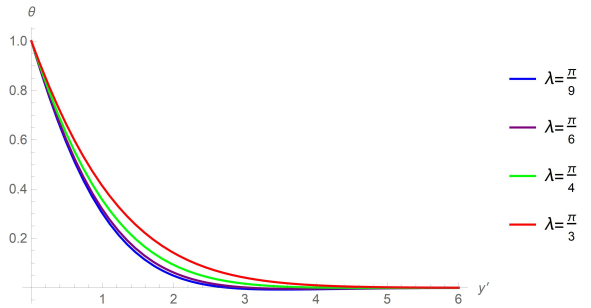


**Figure 15.** Effect of $\lambda$ on temperature profile

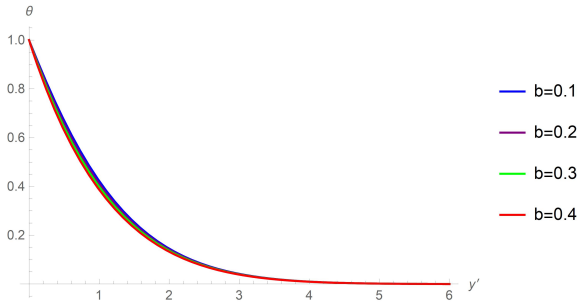


**Figure 16.** Effect of $b$ on temperature profile

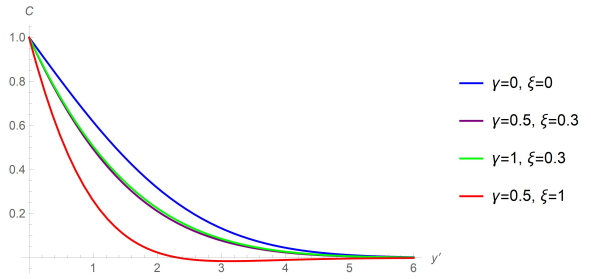


**Figure 17.** Effects of $\gamma$ & $\xi$ on concentration profile

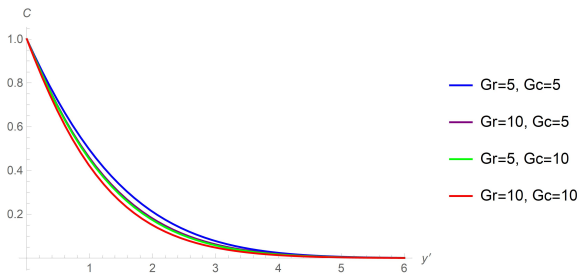


**Figure 18.** Effects of $Gr$ & $Gc$ on concentration profile

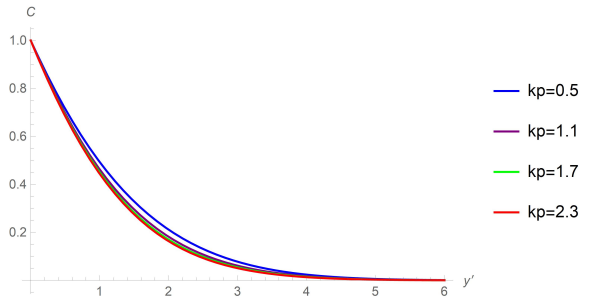


**Figure 19.** Effect of $k_p$ on concentration profile

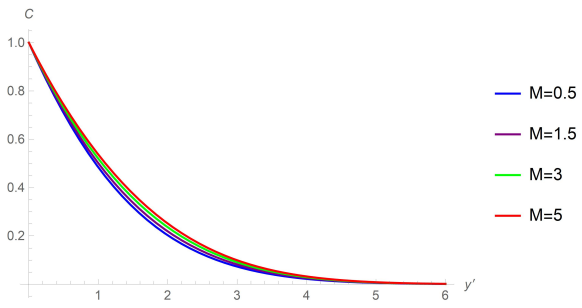


**Figure 20.** Effect of $M$ on concentration profile

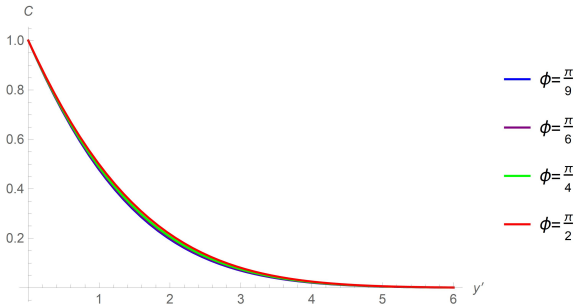


**Figure 21.** Effect of $\phi$ on concentration profile

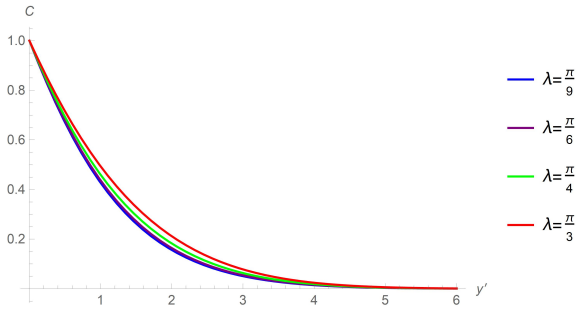


**Figure 22.** Effect of $\lambda$ on concentration profile

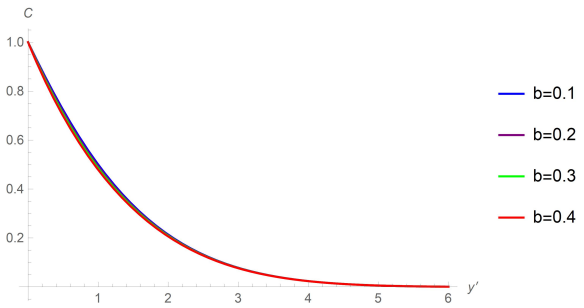


**Figure 23.** Effect of $b$ on concentration profile

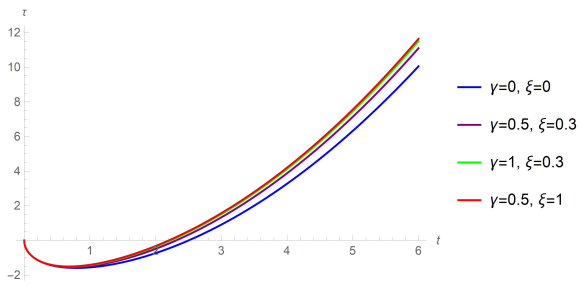


**Figure 24.** Effects of $\gamma$ & $\xi$ on Skin Friction

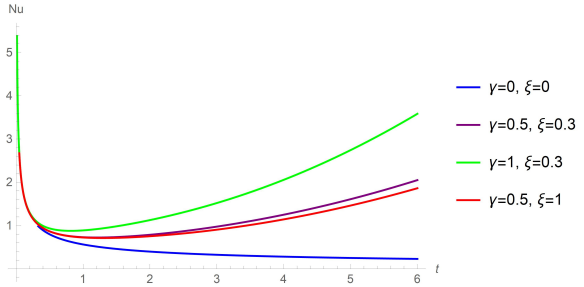


**Figure 25.** Effects of $\gamma$ & $\xi$ on Nusselt Number

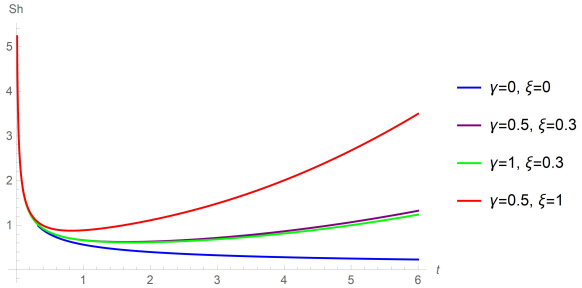


**Figure 26.** Effects of $\gamma$ & $\xi$ on Sherwood Number

**Table 1.** The impact of different parameter on Skin Friction, Nusselt Number and Sherwood Number with $t = 2$, $\gamma = 0.5$ and $\xi = 0.3$

| $M$ | $k_p$ | $Gr$ | $Gc$ | $\phi$ | $\lambda$ | $b$ | $\tau$ | $Nu$ | $Sh$ |
|---|---|---|---|---|---|---|---|---|---|
| 1 | 0.5 | 2 | 2 | $\frac{\pi}{3}$ | $\frac{\pi}{3}$ | 0.2 | 0.692507 | 0.641668 | 0.544578 |
| **3** | 0.5 | 2 | 2 | $\frac{\pi}{3}$ | $\frac{\pi}{3}$ | 0.2 | 1.08778 | 0.604961 | 0.522554 |
| **5** | 0.5 | 2 | 2 | $\frac{\pi}{3}$ | $\frac{\pi}{3}$ | 0.2 | 1.40899 | 0.580339 | 0.50778 |
| 1 | **1.1** | 2 | 2 | $\frac{\pi}{3}$ | $\frac{\pi}{3}$ | 0.2 | 0.323167 | 0.682832 | 0.569276 |
| 1 | **1.7** | 2 | 2 | $\frac{\pi}{3}$ | $\frac{\pi}{3}$ | 0.2 | 0.193087 | 0.698862 | 0.578894 |
| 1 | 0.5 | **5** | 2 | $\frac{\pi}{3}$ | $\frac{\pi}{3}$ | 0.2 | 0.0994802 | 0.715856 | 0.58909 |
| 1 | 0.5 | **10** | 2 | $\frac{\pi}{3}$ | $\frac{\pi}{3}$ | 0.2 | −0.810403 | 0.821675 | 0.652582 |
| 1 | 0.5 | 2 | **5** | $\frac{\pi}{3}$ | $\frac{\pi}{3}$ | 0.2 | 0.073624 | 0.720836 | 0.592079 |
| 1 | 0.5 | 2 | **10** | $\frac{\pi}{3}$ | $\frac{\pi}{3}$ | 0.2 | −0.904434 | 0.840987 | 0.664169 |
| 1 | 0.5 | 2 | 2 | $\frac{\pi}{\mathbf{4}}$ | $\frac{\pi}{3}$ | 0.2 | 0.615765 | 0.649673 | 0.549381 |
| 1 | 0.5 | 2 | 2 | $\frac{\pi}{\mathbf{6}}$ | $\frac{\pi}{3}$ | 0.2 | 0.534835 | 0.658429 | 0.554635 |
| 1 | 0.5 | 2 | 2 | $\frac{\pi}{3}$ | $\frac{\pi}{\mathbf{4}}$ | 0.2 | 0.353811 | 0.684906 | 0.57052 |
| 1 | 0.5 | 2 | 2 | $\frac{\pi}{3}$ | $\frac{\pi}{\mathbf{6}}$ | 0.2 | 0.1008 | 0.716574 | 0.589521 |
| 1 | 0.5 | 2 | 2 | $\frac{\pi}{3}$ | $\frac{\pi}{3}$ | **0.3** | 1.47854 | 0.70505 | 0.582607 |
| 1 | 0.5 | 2 | 2 | $\frac{\pi}{3}$ | $\frac{\pi}{4}$ | **0.4** | 2.26457 | 0.768432 | 0.620636 |

**Table 2.** The influence of $\gamma$ and $\xi$ on $\tau$, $Nu$ and $Sh$

| | $\gamma = 0, \xi = 0$ | $\gamma = 0.5\ \xi = 0.3$ | Change in Percentage |
|---|---|---|---|
| $\tau$ | −0.733082 | −0.488104 | 33.42% ↑ |
| $Nu$ | 0.398942 | 0.788073 | 97.54% ↑ |
| $Sh$ | 0.398942 | 0.632421 | 36.91% ↑ |

## 6. CONCLUSION

This article presents an exact analysis of fluid flow across an inclined parabolic plate inside a permeable medium, considering the influence of an inclined magnetic field, as well as heat and mass stratification. Ultimately, the following conclusions are derived.

- Velocity is diminished as a result of diminished buoyancy forces as thermal ($\gamma$) and mass ($\xi$) stratification increases. Temperature is reduced by thermal stratification, while it is elevated by mass stratification. The concentration of

fluid increases as $\gamma$ increases, while it decreases as $\xi$ decreases. Nusselt number ($Nu$), Sherwood number ($Sh$), and Skin Friction are all enhanced by both $\gamma$ and $\xi$, which also improves heat and mass transfer.

- The velocity is increased by the stronger buoyancy forces that result from higher $Gr$ and $Gc$ values. Temperature and concentration decrease with increasing $Gr$ and $Gc$, indicating enhanced convective cooling. Moderate values improve $Nu$ and $Sh$; very high values may lead to flow reversal near the plate, lowering skin friction.
- Velocity increases with $k_p$ due to improved fluid mobility. Temperature and concentration decrease as permeability increases. Skin friction decreases, while $Nu$ and $Sh$ improve with higher $k_p$.
- Velocity decreases as $M$ increase due to the resistive Lorentz force. Temperature and concentration increase because of resistive heating and flow confinement. Skin friction increases, while $Nu$ and $Sh$ decrease with increasing $M$.
- Higher $\phi$ values decrease velocity by enhancing the Lorentz force. Temperature and concentration rise with increasing $\phi$. Also, Heat and mass transfer improve; skin friction decreases slightly.
- Increasing $\lambda$ reduces velocity due to increased frictional resistance. Temperature and concentration profiles rise with larger plate angles. Also Heat and mass transfer are enhanced; skin friction experiences a minor reduction.
- Velocity increases with $b$ due to stronger propulsive forces. Temperature and concentration decrease due to redistribution of thermal energy. All three quantities—skin friction, $Nu$, and $Sh$—increase with $b$.
- Presence of both stratification leads to:
  - 33.42% increase in skin friction,
  - 97.54% increase in heat transfer rate ($Nu$),
  - 36.91% increase in mass transfer rate ($Sh$).

In our study, the values for $Pr$ and $Sc$ must be taken into consideration as unity in order to have a thorough analysis and make the equations tractable, that is, to discover accurate solutions in closed form. To get a thorough grasp of the model, it is advised that future studies use numerical techniques to find solutions for the coupled equations with different values of $Pr$ and $Sc$. The findings of this study have practical applications in optimizing industrial cooling systems, enhancing heat exchanger efficiency, and improving pollution control strategies. These insights are particularly valuable for engineering and energy systems where precise control of heat and mass transfer is critical.

## ORCID

**Mukul Medhi**, https://orcid.org/0009-0003-2828-0315; **Rudra Kanta Deka**, https://orcid.org/0009-0007-1573-4890

## REFERENCES

[1] H. Alfvén, "Existence of Electromagnetic-Hydrodynamic waves," Nature, **150**(3805), 405-406 (1042). https://doi.org/10.1038/150405d0

[2] P. Caldirola, "Shercliff, J. A. - A Textbook Of Magnetohydrodynamics," Scientia, Rivista di Scienza, **60**(101), 364 (1966).

[3] P.H. Roberts, *An introduction to magnetohydrodynamics*, vol. 6, (Longmans, London, 1967).

[4] V.C. Ferraro and C. Plumpton, *Introduction to magneto-fluid mechanics*, (Oxford University, New York, (1966).

[5] K.R. Cramer and S.-I. Pai, *Magnetofluid dynamics for engineers and applied physicists*, (MacGraw-Hill, New York, 1973)

[6] S. Rashidi, J.A. Esfahani and M. Maskaniyan, "Applications of magnetohydrodynamics in biological systems-a review on the numerical studies," Journal of Magnetism and Magnetic Materials, **439**, 358-372 (2017). https://doi.org/10.1016/j.jmmm.2017.05.014

[7] O.M. Al-Habahbeh, M. Al-Saqqa, M. Safi and T Abo Khater, "Review of magnetohydrodynamic pump applications," Alexandria Engineering Journal, **55**(2), 1347-1358, (2016). https://doi.org/10.1016/j.aej.2016.03.001

[8] K. Ramesh, K.K. Asogwa, R.K. Lodhi, M.I. Khan, M. Medani, K.A. Gepreel and D. Abduvalieva, "Numerical investigation of electroosmotic driven transport of MHD Casson fluid over an exponential stretching sheet using quartic B-spline method," Numerical Heat Transfer, Part A: Applications, 1-16, (2024). https://doi.org/10.1080/10407782.2024.2345864

[9] M.V. Krishna, "Analytical study of chemical reaction, Soret, Hall and ion slip effects on MHD flow past an infinite rotating vertical porous plate," Waves in Random and Complex Media, **35**(2), 2475-2501 (2025). https://doi.org/10.1080/17455030.2022.2044094

[10] M. Kazim, S. Hussain, S. Muhammad and M.A. Abbas, "Analysis of MHD viscous fluid flow under the influence of viscous dissipation force over vertically moving plate with innovative constant proportional caputo derivative," Partial Differential Equations in Applied Mathematics, **14**, 101163 (2025). https://doi.org/10.1016/j.padiff.2025.101163

[11] T. Pradhan, S. Jena and S.R. Mishra, "Laplace transformation technique for free convective time-dependent MHD flow over a vertical porous flat plate with heat sink and chemical reaction: An analytical approach," Hybrid Advances, **8**, 100363 (2025). https://doi.org/10.1016/j.hybadv.2024.100363

[12] Sehra, S.U. Haq, S.I.A. Shah, K.S. Nisar, S.U. Jan and I. Khan, "Convection heat mass transfer and MHD flow over a vertical plate with chemical reaction, arbitrary shear stress and exponential heating," Scientific reports, **11**(1), 4265 (2021). https://doi.org/10.1038/s41598-021-81615-8

[13] B.K. Jha, M.M. Altine and A.M. Hussaini, "MHD steady natural convection in a vertical porous channel in the presence of point/line heat source/sink: An exact solution," Heat transfer, **52**(7), 4880-4894 (2023). https://doi.org/10.1002/htj.22903

[14] S. Sarma and N. Ahmed, "Dufour effect on unsteady MHD flow past a vertical plate embedded in porous medium with ramped temperature," Scientific Reports, **12**(1), 13343 (2022). https://doi.org/10.1038/s41598-022-15603-x

[15] S.R. Yedhiri, K.K. Palaparthi, R. Kodi and F. Asmat, "Unsteady MHD rotating mixed convective flow through an infinite vertical plate subject to Joule heating, thermal radiation, Hall current, radiation absorption," "Journal of Thermal Analysis and Calorimetry," **149**(16), 8813-8826 (2024). https://doi.org/10.1007/s10973-024-12954-7

[16] K. Bhaskar, K. Sharma and K. Bhaskar, "MHD squeezed radiative flow of Casson hybrid nanofluid between parallel plates with joule heating," International Journal of Applied and Computational Mathematics, **10**(2), 80 (2024). https://doi.org/10.1007/s40819-024-01720-w

[17] M. Shareef, "MHD flow along a vertical plate with heat and mass transfer under ramped plate temperature," Jordan Journal of Mechanical & Industrial Engineering, **17**(2), 183-193 (2023). https://doi.org/10.59038/jjmie/170203

[18] K. Raghunath, M. Obulesu and K.V. Raju, "Radiation absorption on MHD free conduction flow through porous medium over an unbounded vertical plate with heat source," International journal of ambient energy, **44**(1), 1712-1720 (2023). https://doi.org/10.1080/01430750.2023.2181869

[19] G.I. Taylor, "A model for the boundary condition of a porous material. Part 1," Journal of Fluid Mechanics, **49**(2), 319-326 (1971). https://doi.org/10.1017/S0022112071002088

[20] S. Richardson, "A model for the boundary condition of a porous material. Part 2," Journal of Fluid Mechanics, **49**(2), 327-336 (1971). https://doi.org/10.1017/S002211207100209X

[21] I. Khan, H. Firdous, S. Alshehery, W.A. Khan, S.M. Husnine and A. Khan, "Effect of heat generation and chemical reaction on convective MHD flow of Jeffrey nanofluids in a porous medium," ZAMM - Journal of Applied Mathematics and Mechanics / Zeitschrift Für Angewandte Mathematik Und Mechanik, **105**(1), e202300877 (2025). https://doi.org/10.1002/zamm.202300877

[22] B.P. Jadhav and S.N. Salunkhe, "Chemically and thermally radiated Williamson MHD fluid over porous media with heat source-sink," International Journal of Modelling and Simulation, **45**(2), 544-558 (2025). https://doi.org/10.1080/02286203.2023.2223401

[23] M. Sheikholeslami, H.R. Kataria, A.S. Mittal, "Effect of thermal diffusion and heatgeneration on MHD nanofluid flow past an oscillating vertical plate through porous medium," Journal of Molecular Liquids, **257**, 12-25 (2018). https://doi.org/10.1016/j.molliq.2018.02.079

[24] M.F. Endalew and S. Sarkar, "Capturing the transient features of double diffusive thin film flow of a second grade fluid through a porous medium," International Journal of Applied and Computational Mathematics, **5**(6), 160 (2019). https://doi.org/10.1007/s40819-019-0743-7

[25] M.V. Krishna, "Diffusion-thermo, thermo-diffusion, hall and ion slip effects on mhd flow through porous medium in a rotating channel," Chemical Physics, **593**, 112623 (2025). https://doi.org/10.1016/j.chemphys.2025.112623

[26] K. Sudarmozhi, D. Iranian, I. Khan and S. Al-Otaibi, "Effects of porous medium in MHD flow of Maxwell fluid with Soret/Dufour impacts," Journal of Porous Media, **27**(4), 23-43 (2024). https://doi.org/10.1615/JPorMedia.2023048112

[27] A. Ali, S. Hussain, M. Ashraf, *et al*., "Theoretical investigation of unsteady MHD flow of Casson hybrid nanofluid in porous medium: Applications of thermal radiations and nanoparticle," Journal of Radiation Research and Applied Sciences, **17**(3), 101029 (2024). https://doi.org/10.1016/j.jrras.2024.101029

[28] H. Nayar and P.A. Phiri, "Investigation of heat and mass transfer of free convective MHD flow along a vertical plate in a porous medium using the new modified differential transform-decomposition method," Results in Engineering, **25**, 104083 (2025). https://doi.org/10.1016/j.rineng.2025.104083

[29] M.F. Endalew, A. Nayak and S. Sarkar, "Flow past an oscillating slanted plate under the effects of inclined magnetic field, radiation, chemical reaction, and time-varying temperature and concentration," International Journal of Fluid Mechanics Research, **47**(3), 247-261 (2020). https://doi.org/10.1615/InterJFluidMechRes.2020026987

[30] M.F. Endalew and A. Nayak, "Thermal radiation and inclined magnetic field effects on MHD flow past a linearly accelerated inclined plate in a porous medium with variable temperature," Heat Transfer - Asian Research, **48**(1), 42-61 (2019). https://doi.org/10.1002/htj.21367

[31] X. Su and Y. Yin, "Effects of an inclined magnetic field on the unsteady squeezing flow between parallel plates with suction/injection," Journal of magnetism and magnetic materials, **484**, 266-271 (2019). https://doi.org/10.1016/j.jmmm.2019.04.041

[32] S. Sadighi, G. Ahmadi, H. Afshar, H.A.D. Ashtiani, and M. Jabbari, "Parametric study of entropy generation in magnetohydrodynamic Casson fluid flow on a porous stretching sheet under an inclined magnetic field," Journal of Applied and Computational Mechanics, **11**(3), 681-691 (2025). https://doi.org/10.22055/jacm.2024.47739.4778

[33] E.M. Nyariki, M.N. Kinyanjui, and P.R. Kiogora, "Unsteady hydro magnetic couette flow in presence of variable inclined magnetic field," International Journal of Engineering Science and Innovative Technology, **6**(2), 2017. https://www.ijesit.com/Volume%206/Issue%202/IJESIT201702_02.pdf

[34] P.T. Hemamalini and M. Shanthi, "Heat and mass transfer on unsteady MHD flow in two nonconducting infinite vertical parallel plates with inclined magnetic field," International Journal of Mechanical Engineering and Technology, **9**(3), 521-536 (2018).

[35] U.S. Rajput and N.K. Gupta, "Dufour effect on unsteady free convection MHD flow past an exponentially accelerated plate through porous media with variable temperature and constant mass diffusion in an inclined magnetic field," International Research Journal of Engineering and Technology, **3**(8), 2135-2140 (2016). https://www.irjet.net/archives/V3/i8/IRJET-V3I8397.pdf

[36] Md.R. Islam, S. Nasrin and Md.M. Alam, "Unsteady MHD fluid flow over an inclined plate, inclined magnetic field and variable temperature with hall and ion-slip current," Ricerche di Matematica, **73**(5), 2477-2504 (2024). https://doi.org/10.1007/s11587-022-00728-y

[37] A. Selvaraj, S.D. Jose, R. Muthucumaraswamy and S. Karthikeyan, "MHD-parabolic flow past an accelerated isothermal vertical plate with heat and mass diffusion in the presence of rotation," Materials Today: Proceedings, **46**, 3546-3549 (2021). https://doi.org/10.1016/j.matpr.2020.12.499

[38] M. Aruna, A. Selvaraj, S.D. Jose and S. Karthikeyan, "Influence on MHD-parabolic flow across a vertical plate is triggered by a rotating fluid with uniform temperature and variable mass diffusion in the absence of hall and Dufour effects," European Chemical Bulletin, **12**, 1123-1132 (2023).

[39] S.D. Jose, A. Selvaraj, R. Muthucumaraswamy, S. Karthikeyan and E. Jothi, "MHD-parabolic flow past an accelerated isothermal vertical plate with variable temperature and uniform mass diffusion in the presence of rotation," in: *Proceedings of First International Conference on Mathematical Modeling and Computational Science: ICMMCS 2020*, (Springer, 2021), pp. 417-428.

[40] M. Umamaheswar, P.C. Reddy, S.H. Reddy, O. Mopuri, and C.K. Ganteda, "Aspects of parabolic motion of MHD fluid flow past a vertical porous plate with cross-diffusion effects," Heat Transfer, **51**(5), 4451-4465 (2022). https://doi.org/10.1002/htj.22507

[41] M. Muralidharan and R. Muthucumaraswamy, "Parabolic started flow past an infinite vertical plate with uniform heat flux and variable mass diffusion," International Journal of Mathematical Analysis, **8**(26), 1265-1274 (2014). http://dx.doi.org/10.12988/ijma.2014.45143

[42] P.C. Reddy, M. Umamheswar, S.H. Reddy, A.B.M. Raju, and M.C. Raju, "Numerical study on the parabolic flow of MHD fluid past a vertical plate in a porous medium," Heat Transfer, **51**(4), 3418-3430 (2022). https://doi.org/10.1002/htj.22457

[43] M.F. Endalew and S. Sarkar, "Incidences of aligned magnetic field on unsteady MHD flow past a parabolic accelerated inclined plate in a porous medium," Heat Transfer, **50**(6), 5865-5884 (2021). https://doi.org/10.1002/htj.22153

[44] K. Chamuah and N. Ahmed, "MHD flow past an impulsively started inclined plate with parabolic plate velocity in the presence of thermal diffusion and thermal radiation," **14**(3), 1-18 (2024). https://doi.org/10.33263/BRIAC143.060

[45] B.S. Goud, P. Srilatha and M.N.R. Shekar, "Study of hall current and radiation effects on MHD free convective flow past an inclined parabolic accelerated plate with variable temperature in a porous medium," Int. J. Mech. Eng. Technol. **9**(7), 1268-1276 (2018).

[46] D. Jose and A. Selvaraj, "Convective heat and mass transfer effects of rotation on parabolic flow past an accelerated isothermal vertical plate in the presence of chemical reaction of first order," JP Journal of Heat and Mass Transfer, **24**(1), 191-206 (2021). http://dx.doi.org/10.17654/HM024010191

[47] A. Shapiro and E. Fedorovich, "Unsteady convectively driven flow along a vertical plate immersed in a stably stratified fluid," Journal of Fluid Mechanics, **498**, 333-352 (2004). https://doi.org/10.1017/S0022112003006803

[48] E. Magyari, I. Pop and B. Keller, "Unsteady free convection along an infinite vertical flat plate embedded in a stably stratified fluid-saturated porous medium," Transport in porous media, **62**, 233-249 (2006). https://doi.org/10.1007/s11242-005-1292-6

[49] C.-Y. Cheng, "Double-diffusive natural convection along a vertical wavy truncated cone in non-newtonian fluid saturated porous media with thermal and mass stratification," International Communications in Heat and Mass Transfer, **35**(8), 985-990 (2008). https://doi.org/10.1016/j.icheatmasstransfer.2008.04.007

[50] C.-Y. Cheng, "Combined heat and mass transfer in natural convection flow from a vertical wavy surface in a power-law fluid saturated porous medium with thermal and mass stratification," International Communications in Heat and Mass Transfer, **36**(4), 351-356 (2009). https://doi.org/10.1016/j.icheatmasstransfer.2009.01.003

[51] H. Kumar and R.K. Deka, "Thermal and mass stratification effects on unsteady flow past an accelerated infinite vertical plate with variable temperature and exponential mass diffusion in porous medium," East European Journal of Physics, (4), 87-97 (2023). https://doi.org/10.26565/2312-4334-2023-4-09

[52] R.S. Nath and R.K. Deka, "Thermal and mass stratification effects on unsteady parabolic flow past an infinite vertical plate with exponential decaying temperature and variable mass diffusion in porous medium," ZAMM-Journal of Applied Mathematics and Mechanics/Zeitschrift für Angewandte Mathematik und Mechanik, **104**(6), e202300475 (2024). https://doi.org/10.1002/zamm.202300475

[53] D. Sahu and R.K. Deka, "Combined impacts of thermal and mass stratification on unsteady MHD parabolic flow along an infinite vertical plate with periodic temperature variation and variable mass diffusion," Heat Transfer, **54**(2), 1638-1649 (2025). https://doi.org/10.1002/htj.23240

[54] R.S. Nath and R.K. Deka, "Thermal and mass stratification effects on MHD nanofluid past an exponentially accelerated vertical plate through a porous medium with thermal radiation and heat source," International Journal of Modern Physics B, **39**(07), 2550045 (2025). https://doi.org/10.1142/S0217979225500456

[55] N. Ahmed, S. Sengupta and D. Datta, "An exact analysis for MHD free convection mass transfer flow past an oscillating plate embedded in a porous medium with Soret effect," Chemical Engineering Communications, **200**(4), 494-513 (2013). https://doi.org/10.1080/00986445.2012.709474

[56] M. Abramowitz and I.A. Stegun, *Handbook of mathematical functions: with formulas, graphs, and mathematical tables*, vol. 55, (Courier Corporation, 1965).

[57] R.B. Hetnarski, "An algorithm for generating some inverse laplace transforms of exponential form," Zeitschrift für angewandte Mathematik und Physik ZAMP, **26**(2), 249-253 (1975). https://doi.org/10.1007/BF01591514

## ТЕПЛО- ТА МАСООБМІН У СТРАТИФІКОВАНІЙ МГД-ТЕЧІЇ ПІД ДІЄЮ ПОХИЛОГО МАГНІТНОГО ПОЛЯ

**Мукул Медхі**, **Рудра Канта Дека**

[a] *Математичний факультет, Університет Гаухаті, Гувахаті-781014, Ассам, Індія*

У цій роботі досліджується, як теплова та масова стратифікація впливають на нестаціонарний магнітогідродинамічний потік рідини через проникне середовище над похилою параболічною пластиною за наявності похилого магнітного поля. Метод перетворення Лапласа використовується для знаходження аналітичних контрольних рішень у замкнутій формі для рівнянь, що описують потік. У дослідженні порівнюються результати, отримані за допомогою теплової та масової стратифікації, зі сценаріями, де обидві форми стратифікації відсутні. Нестратифіковані випадки демонструють підвищені швидкості у порівнянні. Також наявність обох стратифікацій збільшує тертя поверхні на $33,42\%$, швидкість теплопередачі на $97,54\%$ та швидкість масопередачі на $36,91\%$. Найбільший вплив на потік рідини виникає, коли магнітне поле ортогональне до напрямку потоку. Висновки цього дослідження є актуальними для оптимізації гідродинаміки в інженерних та екологічних застосуваннях.

**Ключові слова:** *МГД; пористе середовище; параболічна похила пластина; термічна стратифікація; масова стратифікація; похиле магнітне поле*